Understanding β-Hairpin Formation by Molecular Dynamics Simulations of Unfolding

Jinhyuk Lee and Seokmin Shin*
School of Chemistry and Molecular Engineering, Seoul National University, Seoul 151–747, Korea

ABSTRACT We have studied the mechanism of formation of a 16-residue β-hairpin from the protein GB1 using molecular dynamics simulations in an aqueous environment. The analysis of unfolding trajectories at high temperatures suggests a refolding pathway consisting of several transient intermediates. The changes in the interaction energies of residues are related with the structural changes during the unfolding of the hairpin. The electrostatic energies of the residues in the turn region are found to be responsible for the transition between the folded state and the hydrophobic core state. The van der Waals interaction energies of the residues in the hydrophobic core reflect the behavior of the radius of gyration of the core region. We have examined the opposing influences of the protein-protein (PP) energy, which favors the native state, and the protein-solvent (PS) energy, which favors unfolding, in the formation of the β-hairpin structure. It is found that the behavior of the electrostatic components of PP and PS energies reflects the structural changes associated with the loss of backbone hydrogen bonding. Relative changes in the PP and PS van der Waals interactions are related with the disruption of the hydrophobic core of a protein. The results of the simulations support the hydrophobic collapse mechanism of β-hairpin folding.

INTRODUCTION

The biological functions carried out by proteins are closely related with the unique three-dimensional structures adopted by the linear chains of amino acids. Most small proteins can spontaneously fold to form biologically functional ("native") structures. It was suggested that the information determining the three-dimensional structure is somehow encoded in the amino acid sequence (Anfinsen, 1973). Since Anfinsen's original proposal, there has been a great deal of progress in understanding the "protein-folding" problem. New experimental techniques have provided much information on the details of the events that occur during the folding process (Fersht, 1999; Winkler and Gray, 1998). Theoretical and computational studies of simplified models have provided general insights into the specific features of folding mechanism and the properties of folding free-energy landscapes (Onuchic et al., 1997; Shakhnovich, 1997; Dobson et al., 1998; Dill, 1999). Predicting the native state structures of proteins from amino-acid sequences alone is a long-standing challenge, which has great practical significance as well as considerable scientific interest. Such ab initio structure prediction or protein-folding may require the ability to describe the whole folding process at the level of atomic precision, which is still not feasible despite rapid advances in the field (Duan and Kollman, 1998).

Typical molecular dynamics (MD) simulations can examine the trajectories of proteins up to tens of nanoseconds. The time scales of protein folding in the micro- to millisecond range are still not really accessible to direct simulation studies. A fruitful approach is to investigate protein unfolding by performing simulations under strongly denaturing conditions (high temperature and/or pressure). These simulations can provide insights into the early stages of unfolding, which are assumed to reflect the later stages of refolding under native conditions (Karplus and Sali, 1995; Lazaridis and Karplus, 1997; Wang et al., 1999). It is noted that there remain important open questions concerning the relationship between unfolding at high temperatures and the folding process at physiological temperatures (Finkelstein, 1997; Dinner and Karplus, 1999).

Knowledge of the timescales and mechanism of formation of basic structural elements such as α-helices and β-sheets is essential in understanding the folding of larger proteins. α-helix formation has been extensively investigated both experimentally and theoretically (Muñoz and Serrano, 1995; Williams et al., 1996; Thompson et al., 1997). In contrast, the formation of β-sheet structures has not been studied in detail. It has been proposed that β-turns and β-hairpins act as initiation sites in early protein folding events (Blanco et al., 1998). A β-hairpin is the simplest form of anti-parallel β-sheet structure and is defined by a loop region flanked by two β-strands. Muñoz et al. (1997) studied the kinetics of folding a 16-residue β-hairpin from protein GB1 using a nanosecond laser temperature-jump technique. Folding of the hairpin was found to occur in 6 μs at room temperature, which is ~30 times slower than the rate of α-helix formation. Analysis of the experimental observations suggested that folding of a β-hairpin is stabilized by both hydrogen bonding and hydrophobic interactions and exhibits two-state behavior and a funnel-like, partially rugged energy landscape (Muñoz et al., 1998). This is in contrast to α-helices in which the stability is the result of local residue interactions, mostly the hydrogen bonds. Although the fragment is small, the β-hairpin provides a

Received for publication 6 April 2001 and in final form 9 August 2001.

Address reprint requests to Seokmin Shin, School of Chemistry, and Molecular Engineering, Seoul National University, Seoul 151-747, Korea. Tel: 82-2-880-6639; Fax: 82-2-889-1568; E-mail: sshin@snu.ac.kr.

0006-3495/01/11/2507/10 $2.00

suitable system for investigating fundamental issues in protein folding.

Pande and Rokhsar (1999) studied the unfolding and refolding pathway of a β-hairpin fragment of protein GB1 using MD simulations. They suggested that the high-temperature unfolding of the β-hairpin undergoes a series of sudden discrete conformational changes. These changes occur between states that are identified with the "folded" (*F*), the "hydrophobic core" (*H*), the "partially solvated cluster" (*S*), and the "unfolded" (*U*) states. The states *H* and *S* are obligatory but transient kinetic intermediates. Refolding of the hairpin at low temperatures was studied by a series of short simulations starting from the transition states of the discrete transitions determined by the unfolding simulations. It was found that the transition states determined by the high temperature unfolding and the low temperature refolding simulations showed good agreements.

The work of both Muñoz et al. (1997) and Pande and Rokhsar (1999) concluded that the positioning of the side chain groups in such a way as to promote the formation of the hydrophobic cluster is essential for the folding of the hairpin structure. The primary difference between the two studies is the relative timing of the formations of the interstrand hydrogen bonds near the turn and the hydrophobic core. Two possible mechanisms of β-hairpin folding have been proposed. Muñoz et al. (1997) suggested that the hairpin formation is initiated from the β-turn then "zips up" the remaining native hydrogen bonds. A turn stabilized by interstrand hydrogen bonds positions the aromatic residues so that they are poised to pack into a hydrocarbon cluster. According to Pande and Rokhsar (1999), the hydrophobic cluster would form without assistance from the interstrand hydrogen bonds, suggesting that the β-hairpin refolds by the "hydrophobic collapse" mechanism. In this model, the hairpin collapses to a compact structure associated with a "molten globule." The driving force toward the compact structure is global and in general nonspecific (a hydrophobic interaction). In the next step, "mistakes" in the compact structure are corrected by forming native hydrogen bonds. The reorientation of the compact structure is relatively slow and resembles the transition from a molten globule state to the native state of the protein. Dinner et al. (1999) obtained the free energy surface and conformations involved in the folding of the same β-hairpin from multicanonical Monte Carlo simulations. Their results suggested that folding proceeds by a collapse leading to the formation of the hydrophobic assembly and that then the hairpin hydrogen bonds propagate outwards in both directions from the hydrophobic core. The folding rate is dominated by the time required for interconversion between compact conformations.

Prevost and Ortmans (1997) performed refolding simulations of a β-hairpin fragment of barnase using a simulated annealing method. They found that interstrand side-chain compactness and backbone hydrogen bonding provide concurrent stabilizing factors for the β-hairpin formation. Bonvin and van Gunsteren (2000) studied the stability and folding of the 19-residue β-hairpin fragment of the α-amylase inhibitor tendamistat. Several unfolding and refolding simulations suggested a model for β-hairpin formation in which the turn is formed first, followed by hydrogen bond formation closing the hairpin, and subsequent stabilization by side-chain hydrophobic interactions.

Roccatano et al. (1999) studied the structural and dynamical behavior of the β-hairpin from the protein GB1 at different temperatures using MD simulations in an aqueous environment. The essential dynamics analysis showed that the dynamical behavior of the hairpin at different temperatures, once equilibrated, is very similar and characterized by large motions of the turn and end residues. The results of the simulations provided further evidence of the importance of hydrogen bonds and hydrophobic interactions for the stability of β-hairpin-forming peptides. To understand the balance between backbone and side-chain forces, Ma and Nussinov (2000) studied the contributions of three components of a β-hairpin peptide: turn, backbone hydrogen bonding, and side-chain interactions. They examined the structural stability of the β-hairpin under systematic perturbations of the turn region, backbone hydrogen bonds, and the hydrophobic core formed by the side-chains. It was found that backbone hydrogen bonds are very sensitive to the perturbations and are easily broken. In contrast, the hydrophobic core survives most perturbations. It was shown that hydrophobic interactions were able to keep the peptide folded even with a repulsive force between the β-strands. These results support a side-chain centric view of the folding of a hairpin structure. For small peptides and proteins, the disruption of the hydrophobic core appears to be one of the major steps in the folding/unfolding process. The studies of the mechanical unfolding of the β-hairpin using MD by Bryant et al. (2000) support the view of a stepwise pathway of unfolding, wherein complete breakdown of backbone hydrogen bonds precedes dissociation of the hydrophobic cluster.

In the present study, we have studied unfolding of the β-hairpin from the protein GB1 by MD simulations in explicit water solvents at several temperatures. Unfolding trajectories are analyzed by calculating the order parameters such as the number of hydrogen bonds and the radius of gyration. Further insights into the detailed mechanism of β-hairpin (un)folding are obtained by examining the relative importance of different components of interaction energies. In contrast to α-helices where local interactions due to hydrogen bonding are responsible for the stability, β-hairpins are stabilized by the combining effects of entropy, backbone hydrogen bonding, and interstrand hydrophobic interactions. Previous studies on the hairpins investigated the balance between contributions of different interactions by analyzing the changes in the structural characteristics. The main focus of the present study is to provide direct information about the relative importance of different com-

ponents of interaction energies in the folding mechanism of the hairpin. It is possible to gain valuable information about the formation of β-hairpins by monitoring different interactions during the unfolding simulations. Changes in the interaction energies are also compared with the corresponding behavior of the structural order parameters.

MODEL AND SIMULATION DETAILS

We simulate unfolding of the β-hairpin structure formed by the 16 C-terminal residues (GEWTYDDATKTFTVTE) of protein GB1. The three-dimensional structure of the hairpin is stabilized by the native hydrogen bonds and interactions between the side chains of the four residues (Trp43, Tyr45, Phe52, Val54) forming the hydrophobic core. We have performed simulations with the CHARMM all-H potential (Brooks et al., 1983). The initial structure was taken from the model conformation of the full Protein G (PDB code: 1GB1). The hairpin was placed in a cubic box with the dimension of 37.712 Å, filled with 1728 TIP3P water molecules to a density of $\sim$1 g/cm^3. After removing the water molecules, whose oxygen atoms were within 2.6 Å of any peptide atom, the initial conformation was relaxed by an adapted basis Newton-Raphson method. Bond lengths were constrained through the SHAKE algorithm (Ryckaert et al., 1977). We used time steps of 2 fs for simulations at 300 and 400 K. Smaller time step (1 fs) was used to obtain stable trajectories at higher temperatures (500, 600, and 700 K). Each simulation was started with a heating step from 0 K to the simulation temperature, and further simulations were done for 1 ns (300 and 500–700 K) or 2 ns (400 K). The lengths of simulations are found to be sufficient for observing unfolding processes of the hairpin at 400 to 700 K.

We collected MD trajectories every 5 ps. To analyze the trajectories, we calculated several quantities as order parameters: the number of hydrogen bonds (N_{HB}), the radius of gyration of the hydrophobic core side chains (R_{core}), and the radius of gyration of the whole peptide (R_G). These order parameters are expected to reflect the compactness of the protein structure and give information about the intermediate states of unfolding. The number of hydrogen bonds, N_{HB}, was calculated with the SIMLYS program (Krüger et al., 1991). A hydrogen bond is defined by the bond angle (N—H···O) being restricted in the range between 135° and 180° with the bond distance being less than 3.3 Å.

The overall interaction energy and corresponding force for each residue in a protein can be decomposed into various components. The relative importance of these components can be correlated with conformational changes during the (un)folding of proteins. We have developed a method for calculating different components of the interaction energy or force for each residue in a protein (Lee et al., 2000). For instance, 1) van der Waals (*evdw*), 2) electrostatic (*eelec*), and 3) total (*etot*) interaction energies of each residue with the rest of the protein molecule and solvent molecules can be obtained. We calculated a "protein-protein" (PP) component of energy by summing the average of the total interaction energies of each residue with the solvent coordinates excluded from the trajectories. The difference between the average energy of the whole system and the PP energy can be defined as "protein-solvent" (PS) energy.

RESULTS AND DISCUSSION

We have performed MD simulations of the unfolding of the β-hairpin structure from protein GB1 using CHARMM all-H potential. At high temperatures such as 600 and 700 K, the trajectories of the simulations usually result in a completely unfolded state within 1 ns, whereas the folded states with native-like structures are maintained during the simulations at room temperature (300 K). At an intermediate temperature (400 and 500 K), partial unfolding and refolding of the hairpin are observed in typical trajectories. In Fig. 1, the number of backbone hydrogen bonds N_{HB} for these simulations is shown as a function of time. N_{HB} fluctuates between 4 and 6 at 300 K, reflecting native-like structures. This means that the peptide does not have enough kinetic energy to overcome the barrier between the folded and unfolded states at this temperature. At higher temperatures, the peptide loses the hairpin secondary structure as the backbone-backbone hydrogen bonding is completely broken. Such a structural change corresponds to the transition between the folded state and the hydrophobic core state ($F \rightarrow H$) as proposed by Pande and Rokhsar (1999). It is found that N_{HB} exhibits sharp changes around 500 and 200 ps for the unfolding simulations at 400 and 700 K, respectively. This time of complete breaking of the native hydrogen bonds is identified with the $F \rightarrow H$ transition time.

In Fig. 2, we plot the radius of gyration of the hydrophobic core (Trp43, Tyr45, Phe52, Val54), R_{core}, and the radius of gyration of the whole peptide, R_G, as a function of time. It was suggested that increases in R_{core} characterize the conformational changes associated with the transition between the hydrophobic core state and either the partially solvated (S) or the unfolded (U) state. Neither R_{core} nor R_G change much during the simulations at 300 K. At higher temperatures, sharp changes in the radius of gyration for the hydrophobic core were observed, signaling such transitions between intermediate states. Because the H and S states are transient intermediates, one usually observes reversible interconversions (F $\leftrightarrow$ H $\leftrightarrow$ S $\leftrightarrow$ U) associated with partial unfolding and refolding during simulations at higher temperatures. The analysis of the order parameters, N_{HB} and R_{core}, is consistent with the four-state unfolding mechanism proposed by Pande and Rokhsar (1999). It is noted that discriminating the H and S states based on N_{HB} and the radius of gyration is sometimes difficult. In some cases, the $F \rightarrow H$ and $H \rightarrow S$ transitions cannot be easily separated. The proposed mechanism may be interpreted as the observation that the breaking of the hydrogen bonds precedes the

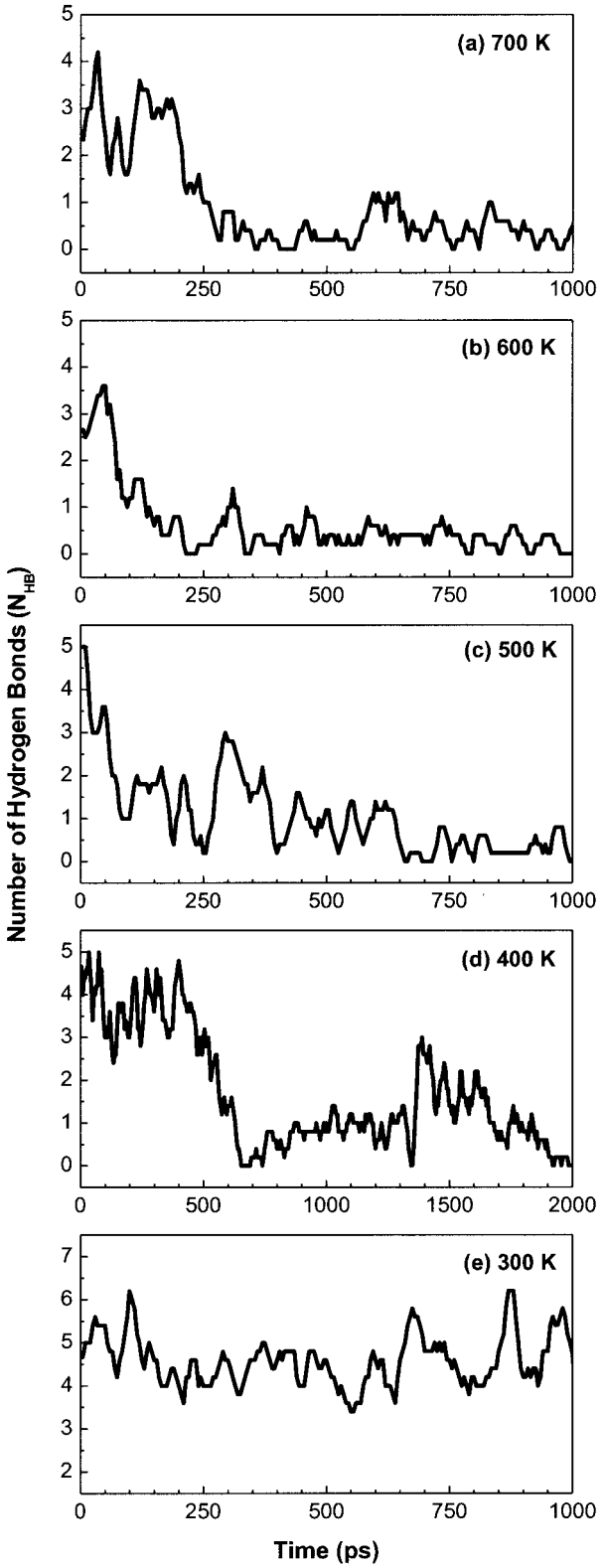

FIGURE 1 The number of hydrogen bonds, N_{HB}, as a function of time for unfolding trajectories at temperatures 700 (*a*), 600 (*b*), 500 (*c*), 400 (*d*), and 300 K (*e*). MD simulations were performed with the CHARMM force field on the β-hairpin structure from protein GB1. The plots have been smoothed by adjacent averaging of 5 points with the raw data sampled once per 5 ps.

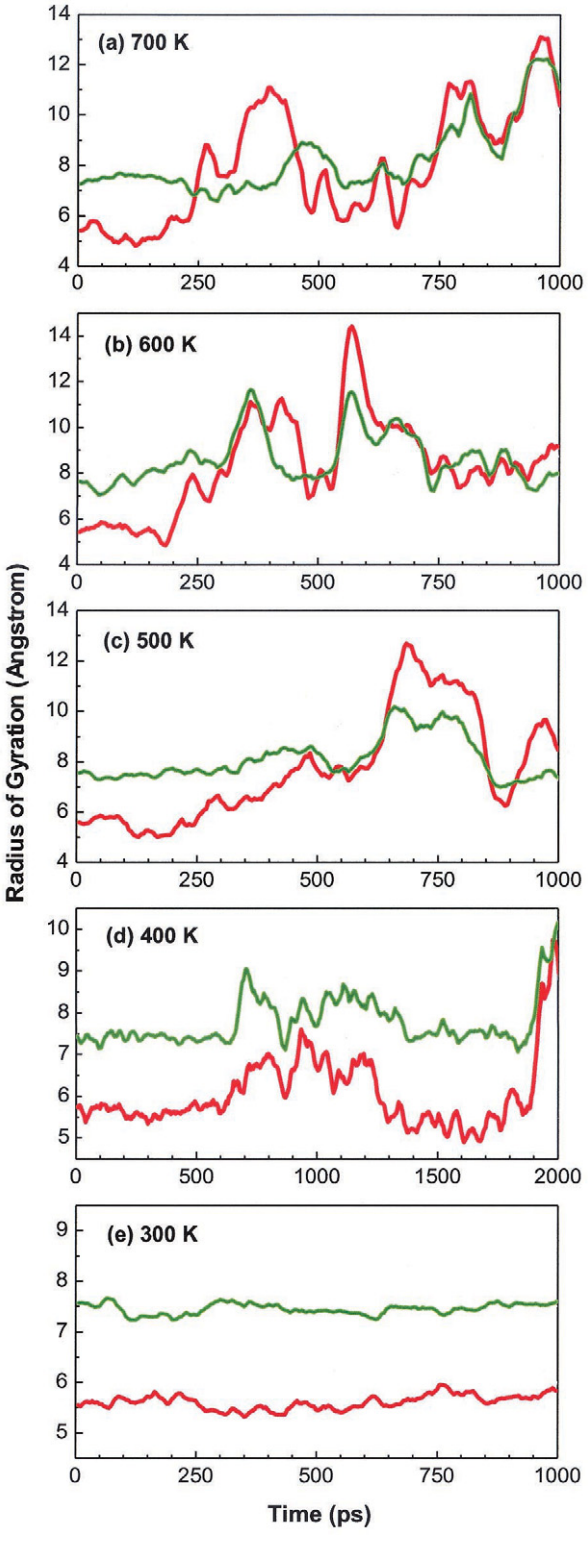

FIGURE 2 The radius of gyration of hydrophobic core, R_{core} (*green line*), and the radius of gyration of peptide, R_G (*red line*), as a function of time for unfolding trajectories at temperatures 700 (*a*), 600 (*b*), 500 (*c*), 400 (*d*), and 300 K (*e*). The plots have been smoothed by adjacent averaging of 5 points with the raw data sampled once per 5 ps.

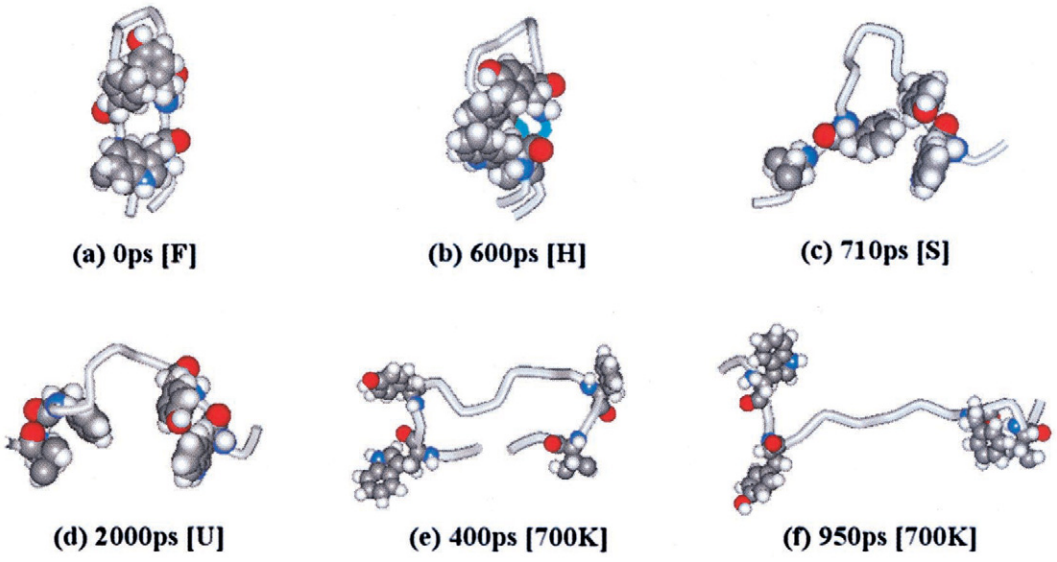

FIGURE 3 MD snapshots showing the unfolding pathway of the β-hairpin. A typical unfolding trajectory at 400 K demonstrates (*a*) the folded state [*F*]; (*b*) the hydrophobic core state [*H*]; (*c*) the partially solvated state [*S*]; (*d*) the unfolded state [*U*]. (*e* and *f*) Conformations of the hairpin with very large core radius of gyration (R_{core}) obtained from the 700-K trajectory. The side chains of the hydrophobic core (Trp43, Tyr45, Phe52, Val54) are shown in space-filling mode.

disruption of the hydrophobic core during the unfolding trajectories. A typical unfolding trajectory at 400 K demonstrating discrete unfolding steps is illustrated in Fig. 3. A complete unfolded state can be characterized by comparable sizes of the core (R_{core}) and the total (R_G) radii of gyration. It is noted that R_{core} was found to be unusually larger than R_G in the time ~400 ps for the simulations at 700 K. This structure, also shown in Fig. 3, is formed by the complete breaking of the hydrophobic core while keeping the two strands at the turn and the terminal region close together. It is different from the extended structure of unfolded states found at 950 ps for the same temperature (Fig. 3). It is not clear how much this intermediate structure may contribute to the (un)folding of the hairpin at lower temperatures.

Various components of interaction energies of residues in a protein can reflect structural changes during (un)folding. We calculated the sum of electrostatic energies (*eelec*) for the six residues in the turn region (residue 46–51). The changes in the electrostatic interactions of these residues show similar behavior as the number of hydrogen bonds during the unfolding trajectories (compare Fig. 4 with Fig. 1). The noticeable differences are found in the later stages of unfolding at 600 and 700 K. Inspection of the actual configurations of the peptide shows that the residues in the turn region are sufficiently close to have relatively large (long-range) electrostatic interactions. The fact that N_{HB} and *eelec* show similar behavior in the transition region between the folded state (*F*) and the hydrophobic core state (*H*) suggests that $F \rightarrow H$ transition involves the breaking the electrostatic interactions of the residues in the turn region. We have also calculated the sum of van der Waals energies (*evdW*) for the residues comprising the hydrophobic core (Trp43, Tyr45, Phe52, Val54). As one might expect, the behavior of *evdW* during unfolding simulations is consistent with the changes in the radius of gyration of the hydrophobic core, R_{core} (compare Fig. 5 with Fig. 2).

The PS energy usually favors the unfolding of a protein, whereas the native state is favored by the PP component of the energy (Boczko and Brooks, 1995). This observation is consistent with the structural features of unfolding: as the protein unfolds, PS interactions occur in preference to the previously favorable PP interactions; the protein becomes more exposed to the solvent, thereby increasing the overall PS energy. We have calculated the electrostatic (*elec*) and the van der Waals (*vdW*) components of PP and PS energies as a function of R_G for unfolding trajectories. Here R_G is taken as a reaction coordinate for protein unfolding. Both components of the PP and PS energies fluctuate around constant values at 300 K. At higher temperatures, the components of PP and PS energies show different behavior depending on the value of R_G.

The relative importance of PP and PS components can change as a protein goes through different states of (un)-folding pathways. In Fig. 6, we compare the *elec* and *vdW* components of PP and PS energies as a function of R_G for the unfolding simulations at 400 K. Changes in PP and PS energies show the opposite behavior in electrostatic interactions. For $R_G > 7.4$, PP electrostatic energy increases sharply to have less negative values, whereas the corresponding PS energy becomes more negative. Similar behavior is observed for the unfolding simulations at 700 K (Fig. 7). This result clearly indicates that the PP electrostatic

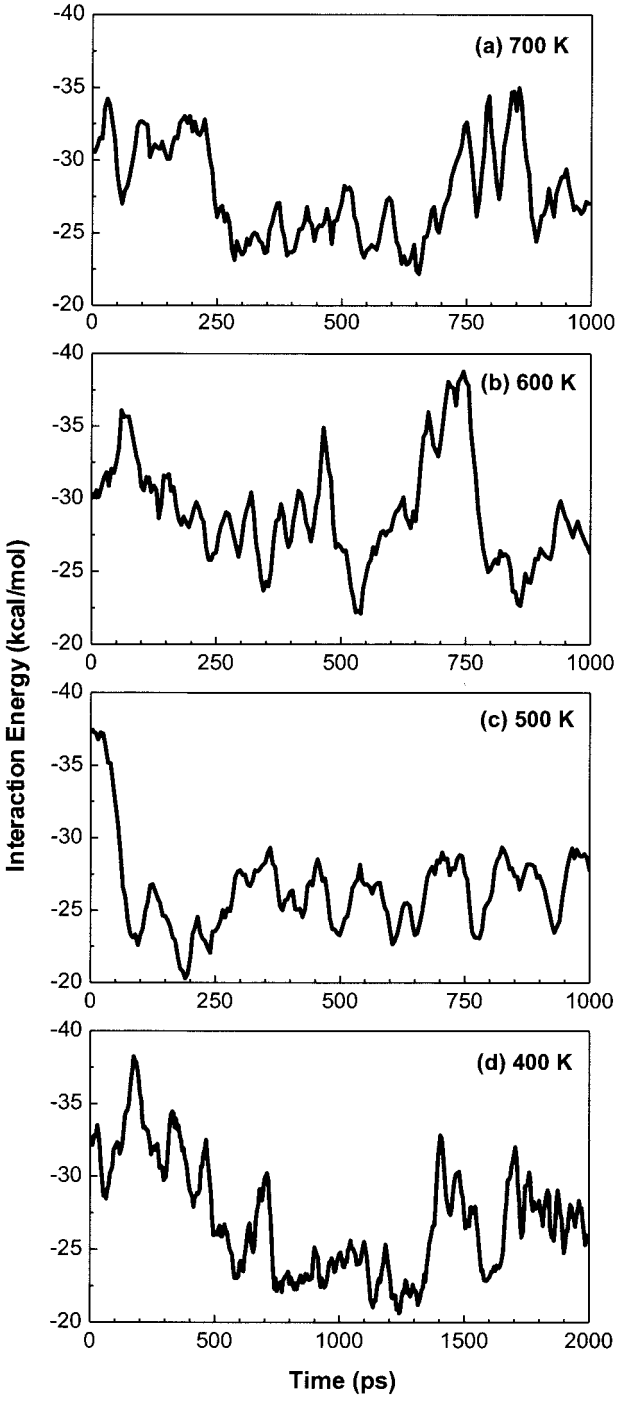

FIGURE 4 The sum of electrostatic energies (*eelec*) for the six residues in the turn region (residue 46–51), plotted as a function of time for unfolding trajectories at temperatures 700 (*a*), 600 (*b*), 500 (*c*), and 400 K (*d*). The plots have been smoothed by adjacent averaging of 5 points with the raw data sampled once per 5 ps.

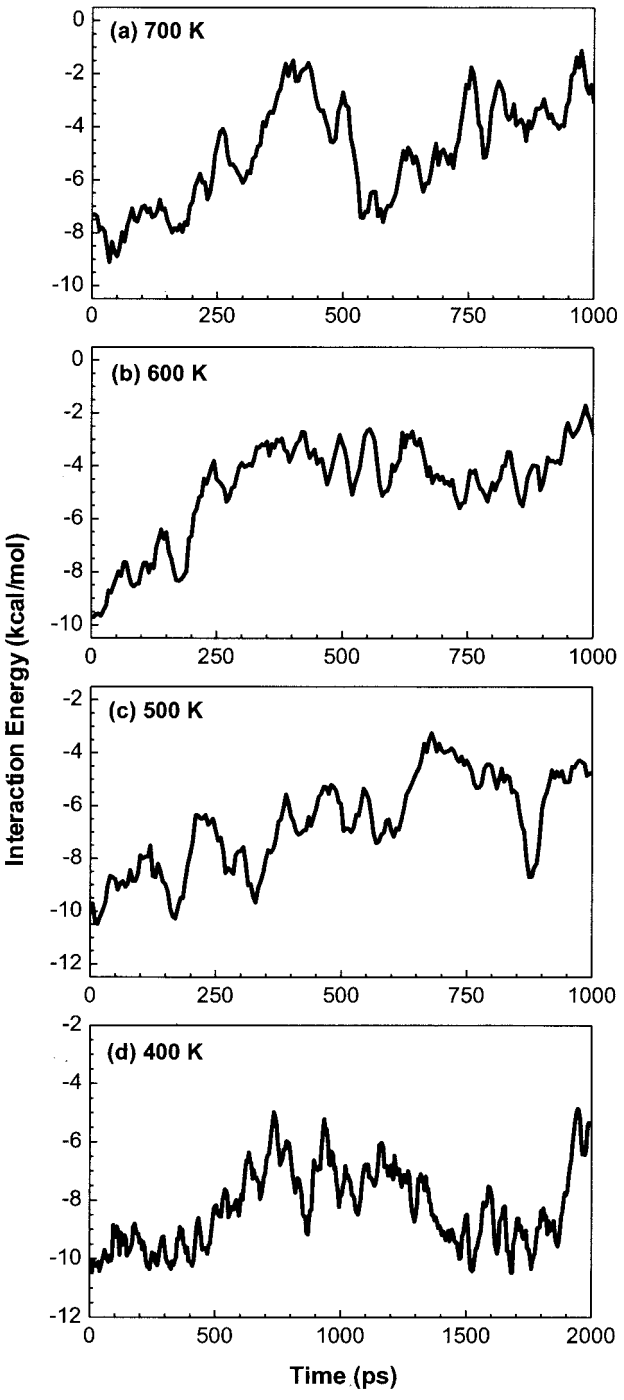

FIGURE 5 The sum of van der Waals energies (*evdW*) for the residues comprising the hydrophobic core (Trp43, Tyr45, Phe52, Val54), plotted as a function of time for unfolding trajectories at temperatures 700 (*a*), 600 (*b*), 500 (*c*), and 400 K (*d*). The plots have been smoothed by adjacent averaging of 5 points, with the raw data sampled once per 5 ps.

interactions, of which backbone hydrogen bonding constitutes a major part, are replaced by hydrogen bonding between the residues and water molecules. In other words, the relative changes of the electrostatic components of PP and PS energies can be related to the loss of backbone hydrogen bonds.

By reasoning similar to the above, the relative changes in the van der Waals (*vdW*) components of PP and PS energies

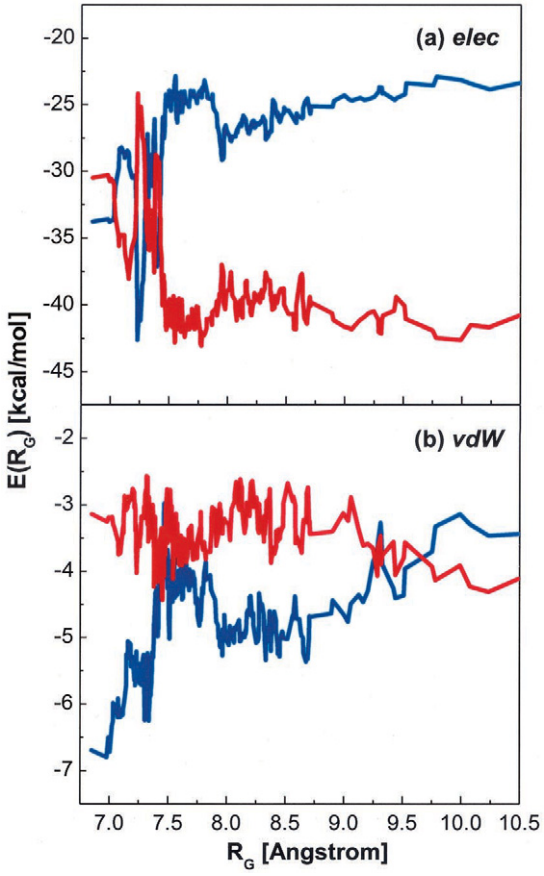

FIGURE 6 Comparison of (*a*) the electrostatic [*elec*] and (*b*) the van der Waals [*vdW*] components of the PP (*blue line*) and the PS (*red line*) energies, plotted as a function of the radius of gyration (R_G). The data are obtained from the unfolding trajectory at 400 K, and the plots have been smoothed by adjacent averaging of 5 points.

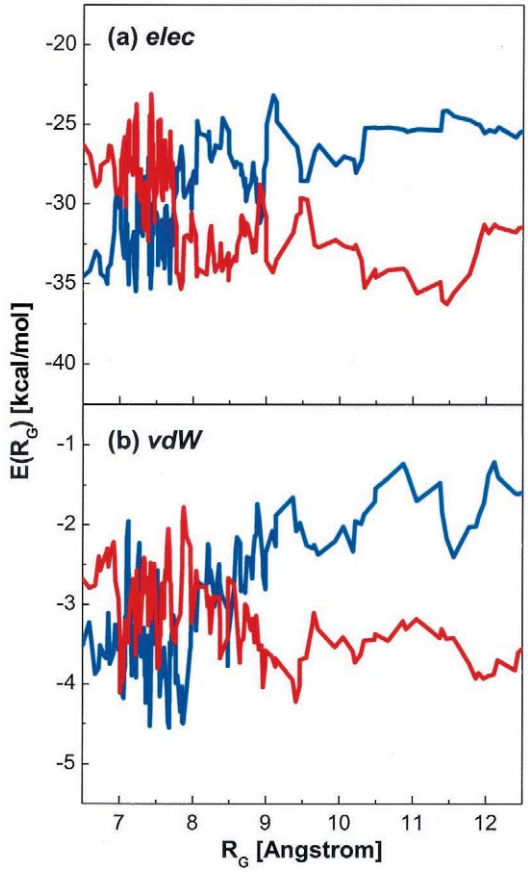

FIGURE 7 Comparison of (*a*) the electrostatic [*elec*] and (*b*) the van der Waals [*vdW*] components of the PP (*blue line*) and the PS (*red line*) energies, plotted as a function of the radius of gyration (R_G). The data are obtained from the unfolding trajectory at 700 K, and the plots have been smoothed by adjacent averaging of 5 points.

can reflect the behavior of hydrophobic interactions during (un)folding processes. In the range of $6.5 < R_G < 7.5$, *vdW* contributions to PP energy get smaller, whereas the corresponding PS energies do not show much drift (Fig. 6 *b*). This energy change is associated with the loosening of the internal structure of the peptide with the breaking of backbone hydrogen bonding. The behavior of PP and PS *vdW* interactions for $R_G > 8.5$ can be related to the opening of the two strands due to the breaking of the hydrophobic cluster. The difference in *vdW* components of PP and PS energies is more clearly seen from the simulations at 700 K as shown in Fig. 7.

In Fig. 8, we plot the electrostatic components of PP and PS as a function of the number of backbone hydrogen bonds. As shown in Fig. 1, the transition between the folded state and the hydrophobic core state is associated with a sharp decrease in N_{HB} ($4 \rightarrow 0$ at 400 K and $3 \rightarrow 0$ at 700 K). Fig. 8 shows that such changes in N_{HB} are related to opposite trends in the changes of PP and PS energies. This result confirms the conclusion that the behavior of the electrostatic components of PP and PS energies reflects the loss of backbone hydrogen bonds.

The analysis on the components of PP and PS energies is consistent with the stepwise unfolding pathway discussed above. The behavior of the electrostatic component of the energies can be related to the $F \leftrightarrow H$ transition and the interconversions between *H*, *S*, and *U* states involve the changes in the relative contributions of the van der Waals interactions. In particular, the results support the mechanism that a complete breakdown of backbone hydrogen bonds precedes disruption of the hydrophobic core during the unfolding of the hairpin structure.

Experimental studies on the formation and stability of β-hairpin structures have been done by different groups (Blanco et al., 1998). Blanco et al. (1994) and Blanco and Serrano (1995) studied the 16 C-terminal residue peptide of protein GB1 by Nuclear Magnetic Resonance (NMR) techniques and showed that a native-like β-hairpin structure is stable in aqueous solution. It was found by the nuclear Overhauser effect spectroscopy (NOESY) experiments that the peptide folds into a β-hairpin conformation with a

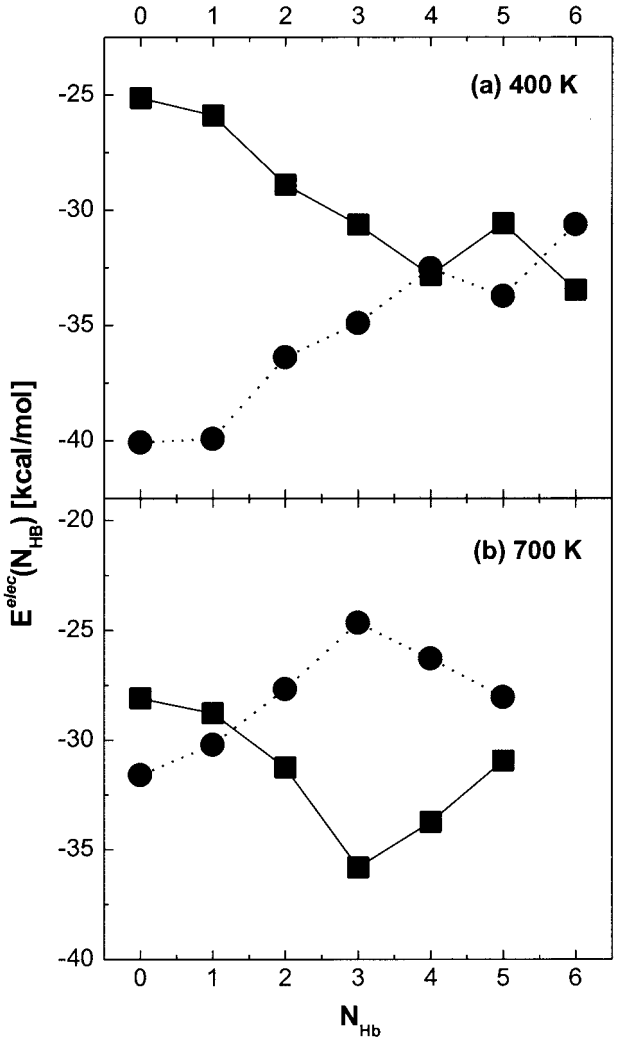

FIGURE 8 Comparison of the electrostatic components of the PP (■) and the PS (●) energies, plotted as a function of the number of hydrogen bonds (N_{HB}). The data are obtained from the unfolding trajectory at temperatures 400 (*a*) and 700 K (*b*).

six-residue turn (46–51) and the three aromatic side chains from the residues of Trp43, Tyr45, and Phe52 become closer to form a hydrophobic core. Kinetic studies of the folding/unfolding of the same peptide by Muñoz et al. (1997) were based on the observation that the fluorescence of the Trp43 increases due to the stabilization in a hydrophobic cluster formed by three other residues (Tyr45, Phe52, Val54). Theses findings are consistent with the results of the present simulations where the formation of the hydrophobic core is shown to be responsible for the stability of the β-hairpin structure.

As discussed in the Introduction, the β-hairpin structures from different proteins seemed to follow different mechanism of folding. The present study and other studies suggest that the β-hairpin fragment of protein GB1 folds by the hydrophobic collapse mechanism where the formation of

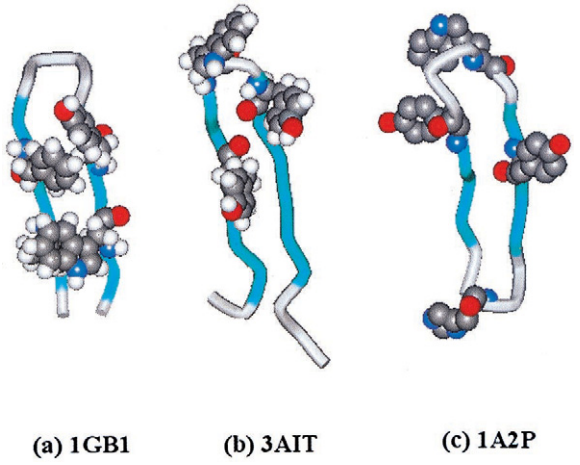

FIGURE 9 Comparison of native structures of the β-hairpin fragments from (*a*) the protein GB1 (residues 41–56 of 1GB1), (*b*) the α-amylase inhibitor tendamistat (residues 10–28 of 3AIT), and (*c*) the barnase (residues 85–102 of 1A2P). The side chains of hydrophobic residues ((Trp43, Tyr45, Phe52, Val54) of 1GB1; (Tyr15, Trp18, Tyr20) of 3AIT; and (Tyr90, Trp94, Tyr97, His102) of 1A2P) are shown in space-filling mode.

the hydrophobic assembly is followed by the propagation of the backbone hydrogen bonds outwards in both directions from the hydrophobic core. The folding of the 19-residue β-hairpin fragment of the α-amylase inhibitor tendamistat was found to follow different mechanism in which the turn is formed first, followed by hydrogen bond formation closing the hairpin, and subsequent stabilization by side-chain hydrophobic interactions (Bonvin and van Gunsteren, 2000). In the case of a β-hairpin fragment of barnase, it was found that all the observed increases in compactness due to the hydrophobic interactions occur simultaneously with the formation of a backbone hydrogen bond during the refolding simulations (Prevost and Ortmans, 1997).

In a recent study on the thermodynamics and kinetics of off-lattice models for the β-hairpin fragment, Klimov and Thirumalai (2000) suggested that the basic mechanisms of folding depend on the intrinsic rigidity of the hairpin, which is determined by the location of the hydrophobic cluster. In Fig. 9, the folded structures of the three β-hairpin fragments discussed above are compared. It is clear that the positions of the large (hydrophobic) side-chains are different in the three cases. In the β-hairpin of protein GB1, the hydrophobic residues are located in the middle of the two strands. The stability and the initial folding of the peptide are dominated by the formation of the hydrophobic core. The β-hairpin of tendamistat has the hydrophobic residues clustered near the turn (loop) region, which facilitates the early formation of the turn and the subsequent hydrogen bond formation closing the hairpin. For the hairpin of barnase, the hydrophobic residues do not seem to form a cluster around one region of the peptide. The best way of folding in this case would be the formation of hydrogen bonds assisted by the concomitant side-chain hydrophobic interactions. Systematic

(un)folding simulations on these different hairpin fragments are expected to provide valuable information about the stability and formation of β-hairpin structures, which will be the subject of future studies.

CONCLUSION

We have studied the mechanism of a β-hairpin formation by unfolding simulations at high temperatures. The analysis of trajectories obtained from MD simulations in explicit aqueous solution suggests a refolding pathway consisting of several transient intermediates. The behavior of the order parameters such as the number of backbone hydrogen bonds (N_{HB}) and the radius of gyration of the hydrophobic core (R_{core}) is consistent with the four-state discrete unfolding mechanism proposed by Pande and Rokhsar (1999).

The changes in the interaction energies of residues can be related with the structural changes during the unfolding of the hairpin. The electrostatic energies of the residues in the turn region show similar behavior as the number of backbone hydrogen bonds. The breaking of the electrostatic interactions of such residues is responsible for the transition between the folded state and the hydrophobic core state. The van der Waals interaction energies of the residues in the hydrophobic core reflect the behavior of the radius of gyration of the core region.

Understanding the relative importance of different components of interaction energies during the (un)folding of a protein can provide valuable information. We have studied possible correlations between relative changes in the PP and PS energies and the mechanism of protein folding. It is found that the PP component of energy favors the native-like states and the unfolding process is favored by the PS component. Comparison of the electrostatic components of PP and PS energies can reflect the structural changes associated with the loss of backbone hydrogen bonding. Relative changes in the van der Waals components of PP and PS energies are related with the disruption of the hydrophobic core of a protein. The results of the simulations are consistent with the hydrophobic collapse mechanism of β-hairpin folding, whereby the formation of a hydrophobic assembly is followed by a final tune-up for the secondary structure through forming hydrogen bonds in the backbone strand.

This work was supported by the Korea Research Foundation grant through the Research Institute of Basic Sciences of SNU (KRF-2000-0409-20000064). J.L. acknowledges the BK21 fellowship from the Chemistry and Molecular Engineering Division.

REFERENCES

Anfinsen, C. B. 1973. Priciples that govern the folding of protein chains. *Science.* 181:223–230.

Blanco, F., M. Ramírez-Alvarado, and L. Serrano. 1998. Formation and stability of beta-hairpin structures in polypeptides. *Curr. Opin. Struct. Biol.* 8:107–111.

Blanco, F. J., G. Rivas, and L. Serrano. 1994. A short linear peptide that folds into a native stable beta-hairpin in aqueous solution. *Nat. Struct. Biol.* 1:584–590.

Blanco, F. J., and L. Serrano. 1995. Folding of protein G B1 domain studied by the conformational characterization of fragments comprising its secondary structure elements. *Eur. J. Biochem.* 230:634–649.

Boczko, E. M., and C. L. Brooks, III. 1995. First-principles calculation of the folding free energy of a three-helix bundle protein. *Science.* 269: 393–396.

Bonvin, A. M. J. J., and W. F. van Gunsteren. 2000. β-Hairpin stability and folding: molecular dynamics studies of the first β-hairpin of tendamistat. *J. Mol. Biol.* 296:255–268.

Brooks, B. R., R. E. Bruccoleri, B. D. Olafson, D. J. States, S. Swaminathan, and M. Karplus. 1983. CHARMM: a program for macromolecular energy, minimization, and dynamics calculations. *J. Comp. Chem.* 4:187–217.

Bryant, Z., V. S. Pande, and D. S. Rokhsar. 2000. Mechanical unfolding of a beta-hairpin using molecular dynamics. *Biophys. J.* 78:584–589.

Dill, K. A. 1999. Polymer principles and protein folding. *Protein Sci.* 8:1166–1180.

Dinner, A. R., and M. Karplus. 1999. Is protein unfolding the reverse of protein folding: a lattice simulation analysis. *J. Mol. Biol.* 292:403–419.

Dinner, A. R., T. Lazaridis, and M. Karplus. 1999. Understanding beta-hairpin formation. *Proc. Natl. Acad. Sci. U.S.A.* 96:9068–9073.

Dobson, C. M., A. Sali, and K. M. 1998. Protein folding: a perspective from theory and experiment. *Angew. Chem. Int. Ed.* 37:868–893.

Duan, Y., and P. A. Kollman. 1998. Pathways to a protein folding intermediate observed in a 1-microsecond simulation in aqueous solution. *Science.* 282:740–744.

Fersht, A. 1999. Structure and Mechanism in Protein Science. Freeman, New York.

Finkelstein, A. V. 1997. Can protein unfolding simulate protein folding? *Protein Eng.* 10:843–845.

Karplus, M., and A. Sali. 1995. Theoretical studies of protein folding and unfolding. *Curr. Opin. Struct. Biol.* 5:58–73.

Klimov, D. K., and D. Thirumalai. 2000. Mechanisms and kinetics of beta-hairpin formation. *Proc. Natl. Acad. Sci. U.S.A.* 97:2544–2549.

Krüger, P., M. Luke, and A. Szameit. 1991. SIMLYS-a software package for trajectory analysis of molecular dynamics simulations. *Comp. Phys. Commun.* 62:371–380.

Lazaridis, T., and M. Karplus. 1997. "New view" of protein folding reconciled with the old through multiple unfolding simulations. *Science.* 278:1928–1931.

Lee, J., K. Lee, and S. Shin. 2000. Theoretical studies of the response of a protein structure to cavity-creating mutations. *Biophys. J.* 78: 1665–1671.

Ma, B., and R. Nussinov. 2000. Molecular dynamics simulations of a beta-hairpin fragment of protein G: balance between side-chain and backbone forces. *J. Mol. Biol.* 296:1091–1104.

Muñoz, V., E. R. Henry, J. Hofrichter, and W. A. Eaton. 1998. A statistical mechanical model for beta-hairpin kinetics. *Proc. Natl. Acad. Sci. U.S.A.* 95:5872–5879.

Muñoz, V., and L. Serrano. 1995. Helix design, prediction and stability. *Curr. Opin. Biotechnol.* 6:382–386.

Muñoz, V., P. A. Thompson, J. Hofrichter, and W. A. Eaton. 1997. Folding dynamics and mechanism of beta-hairpin formation. *Nature.* 390: 196–199.

Onuchic, J. N., Z. Luthey-Schulten, and P. G. Wolynes. 1997. Theory of protein folding: the energy landscape perspective. *Ann. Rev. Phys. Chem.* 48:545–600.

Pande, V. S., and D. S. Rokhsar. 1999. Molecular dynamics simulations of unfolding and refolding of a beta-hairpin fragment of protein G. *Proc. Natl. Acad. Sci. U.S.A.* 96:9062–9067.

Prevost, M., and I. Ortmans. 1997. Refolding simulations of an isolated fragment of barnase into a native-like beta hairpin: evidence for compactness and hydrogen bonding as concurrent stabilizing factors. *Proteins Struct. Funct. Genet.* 29:212–227.

Roccatano, D., A. Amadei, A. Di Nola, and H. J. Berendsen. 1999. A molecular dynamics study of the 41–56 beta-hairpin from B1 domain of protein G. *Protein Sci.* 8:2130–2143.

Ryckaert, J.-P., G. Ciccotti, and H. J. C. Berendsen. 1977. Numerical integration of the Cartesian equations of motion of a system with constraints: molecular dynamics of n-alkanes. *J. Comp. Phys.* 23: 327–341.

Shakhnovich, E. I. 1997. Theoretical studies of protein-folding thermodynamics and kinetics. *Curr. Opin. Struct. Biol.* 7:29–40.

Thompson, P. A., W. A. Eaton, and J. Hofrichter. 1997. Laser temperature jump study of the helix<==>coil kinetics of an alanine peptide interpreted with a 'kinetic zipper' model. *Biochemistry.* 36:9200–9210.

Wang, L., Y. Duan, R. Shortle, B. Imperiali, and P. A. Kollman. 1999. Study of the stability and unfolding mechanism of BBA1 by molecular dynamics simulations at different temperatures. *Protein Sci.* 8:1292–1304.

Williams, S., T. P. Causgrove, R. Gilmanshin, K. S. Fang, R. H. Callender, W. H. Woodruff, and R. B. Dyer. 1996. Fast events in protein folding: helix melting and formation in a small peptide. *Biochemistry.* 35: 691–697.

Winkler, J. R., and H. B. Gray. 1998. Protein folding special issue. *Acc. Chem. Res.* 31:697–780.